Astron. Astrophys. 139, 171–180 (1984)

ASTRONOMY AND ASTROPHYSICS

IR observations of OH/IR stars

J. Herman [1] *, R. Isaacman [1] **, A. Sargent [2], and H.J. Habing [1]

[1] Sterrewacht Leiden, Postbus 9513, 2300 RA Leiden, The Netherlands
[2] California Institute of Technology 102–24, Pasadena, CA 91125, USA

Received March 8, accepted May 24, 1984

Summary. Results of broad band photometry in eight bands between $\lambda = 3.8\,\mu$m and 20 μm for a number of OH/IR stars are presented. Combination with other available infrared and radio data yields good estimates of the mean luminosities for these (very) long-period variables. Only a small fraction have large luminosities, in excess of $10^4\,L_\odot$, but most OH/IR stars have luminosities comparable to those of the classical Mira variables. The depth of the 9.7 μm silicate feature, the infrared colour temperature, and the mass loss rate are indicative of the strength of the OH maser. A few objects seem radically different in character from the usual OH/IR stars. They are not variable and appear to be nearby low mass stars with a very large mass loss rate.

Key words: Infrared sources – OH masers – stars: (very) long period variables

1. Introduction

For a large number of OH/IR stars we have an extensive data base of radio observations containing information about the variability of the stars and the sizes of the OH shells (Herman and Habing, 1984a). For a smaller set of stars, we also possess knowledge about the brightness distribution, the structure, and the density of the OH envelope (Herman et al., 1984). By combining "phase lag" radii, derived from the light travel times between the front and the back sides of the shell, with the angular extents measured from VLA maps we could determine, in a very direct manner, distances to an accuracy of ~10%. Measurements of the apparent bolometric magnitudes thus yield good absolute luminosities for this limited sample of OH/IR stars.

The spectral energy distribution of OH/IR stars peaks in the near infrared, typically at wavelengths between 2 μm and 10 μm. A considerable fraction of the energy is radiated longward of 10 μm (cf. Werner et al., 1980). Therefore observations out to at least $\lambda = 20\,\mu$m are required to obtain the luminosities of these stars. We have measured a number of OH/IR stars with accurately known radio positions in eight bands between $\lambda = 3.8\,\mu$m and 20 μm. Luminosities in this wavelength range have been determined and estimates of the total luminosities, corrected for variability and interstellar absorption. The relationships between the near infrared colour temperatures, the strength of the 9.7 μm silicate feature and the fraction of luminosity converted into OH luminosity are examined.

Send offprint requests to: J. Herman

* Present address: ESTEC, Postbus 299, 2200 AG Noordwijk zh, The Netherlands

** Present address: Applied Research Corporation, 8201 Corporate Dr., Landover, MD 20785, USA

2. Observations and reduction

We used the 3.8 m United Kingdom Infrared Telescope on Mauna Kea, Hawaii (UKIRT) on June 25–28, 1982 to observe some 25 OH/IR stars. We had good positions for all objects, mostly from VLA measurements; this is a considerable advantage, as serious confusion problems can arise, especially in the galactic plane around the crowded regions at $l \simeq 30°$ (see Jones et al., 1982). Broad band photometry was carried out at the f/35 focus, using a helium-cooled Ge:Ga bolometer with a 7.″5 aperture. Sky subtraction was accomplished by chopping 30″ in declination. The central wavelengths and the bandwidths of the filters are listed in Table 1, together with the conversion factors to Jy ($10^{-26}\,\mathrm{Wm^{-2}\,Hz^{-1}}$) for a 0.m0 star (see Beckwith et al., 1976; cf. Johnson, 1966, or Wamsteker, 1981).

The integration times for each star ranged from 24 to 160 s per band. For calibration standards we used α Sco, α Boo, β Peg, and occasionally some other bright stars (see Appendix A).

3. Results

The energy distributions are displayed in Figs. 1–10, and the observed fluxes in each band are given in Appendix A. Note the

Table 1.

	Band	λ (μm)	Δλ (μm)	F_ν Jy
Bolometer	L'	3.82	0.65	238
	M	4.78	0.60	153
		8.7	1.2	50
		9.7	1.0	40
	N	10.3	1.25	34
		11.6	1.17	28
		12.5	1.25	24
	Q	20.0	6.0	10

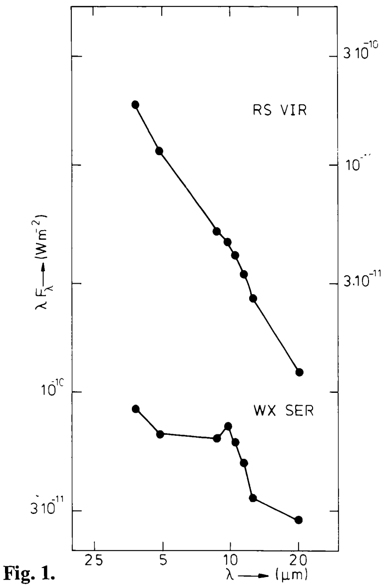

Fig. 1.

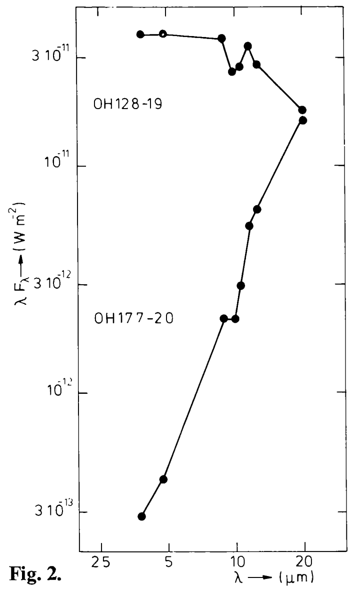

Fig. 2.

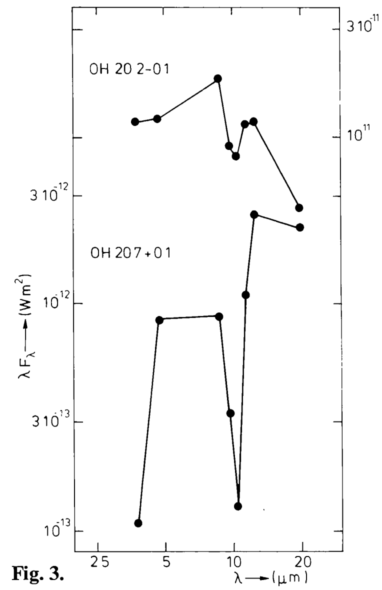

Fig. 3.

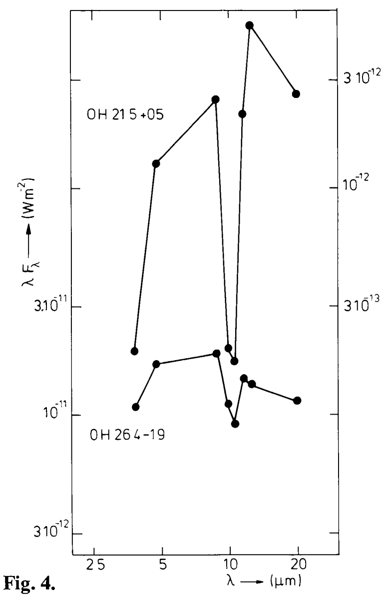

Fig. 4.

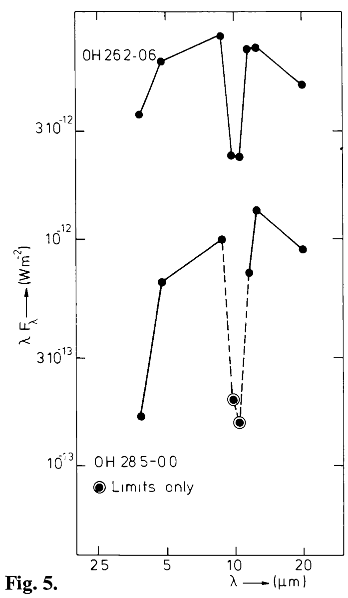

Fig. 5.

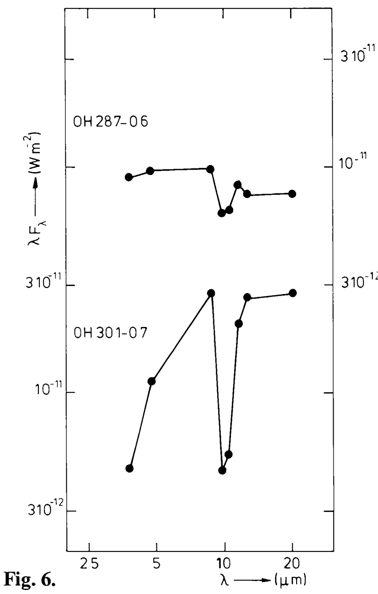

Fig. 6.

large difference between the two Mira variables, WX Ser and RS Vir, where the 9.7 μm feature is seen in emission, and the OH/IR stars that show absorption, sometimes very deep, at 9.7 μm. The very unusual spectrum of OH 17.7–2.0, for which we had a very good position, was confirmed recently by Engels (private communication). Although this shape is unique in our sample, preliminary IRAS data show that more similar cases of such red energy distributions exist (Olnon et al., 1984).

Other pertinent results are given in Table 2, where in column 1 the names are listed. Column 2 contains information about the positions. The VLA positions (references *b–d*) are very accurate ($\lesssim 1''$), the others less so ($\lesssim 5''$). In Columns 3 and 4 the radio periods and the phases (Herman and Habing, 1984a, Table 3) are given. The distances, their uncertainties, and a reference to the manner of their determination are listed in Columns 5–7. The geometric distances (2), derived directly from the comparison of the "phase lag" radii with the angular extents (Herman et al., 1983, Table 3), are very good (10–20 %). The distances marked by (3) have been found from a relation between the absolute OH luminosity and the OH radius (Herman and Habing, 1984b). They are less certain (~ 30 %, depending on the accuracy of the phase lag measurement). When the phase lag was poorly determined, we took the harmonic mean of the near kinematic distance and the distance derived as just described. In these cases the errors can be considerable, and no uncertainties are tabulated. For the two Mira variables we took the mean of the distances from Robertson and Feast (1981, based on a period-luminosity relation), from Rieu et al. (1979, based on m_v at maximum), and from a method of our own (based on an absolute *K* magnitude of $2^{m}.1$; see Herman and Habing, 1984b, Sect. 5.a1). For RS Vir the three different methods yield quite similar distances; for WX Ser, however, there is a large discrepancy (~ 1 kpc).

The luminosities presented in column 8 were determined by integrating the energy distribution from 3.8 μm to 20 μm, allowing for a *25 % correction* for the flux emitted at wavelengths longward of 20 μm. This correction is in accord with the 20 % used by Werner

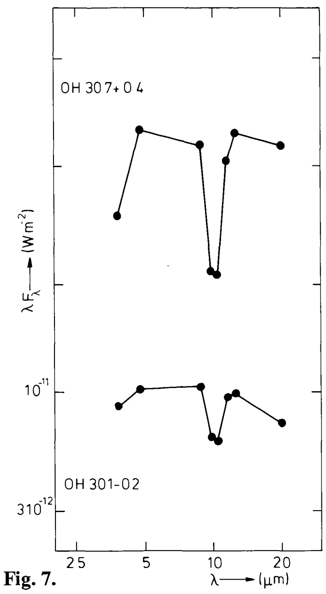

Fig. 7.

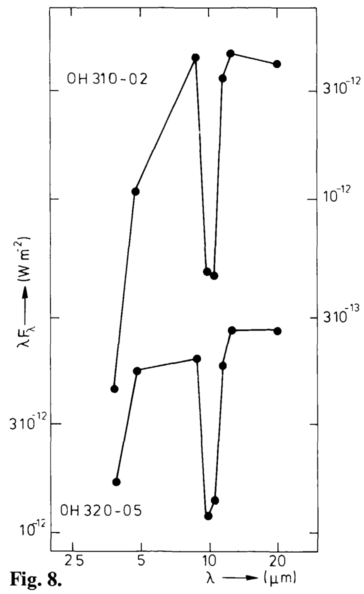

Fig. 8.

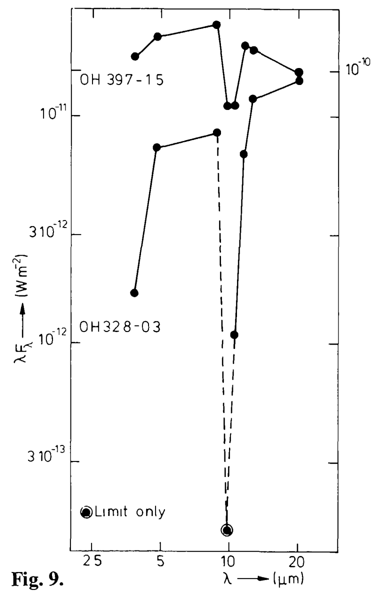

Fig. 9.

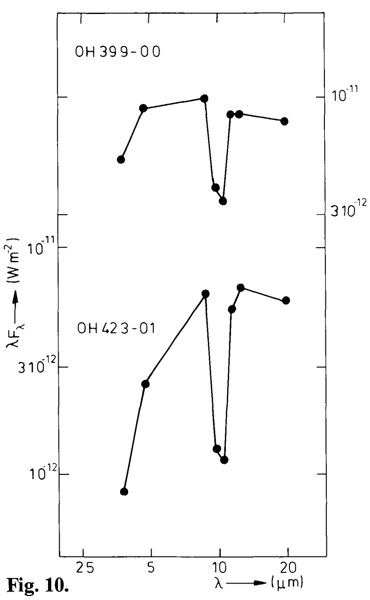

Fig. 10.

Figs. 1–10. Spectra of 1612 MHz OH masers observed with UKIRT. Where two scales are given, the scale on the right refers to the upper spectrum

et al. (1980) for the flux at $\lambda > 25\,\mu$m. The sources with geometric distances are underlined (Columns 8 and 9). The colour temperature between $\lambda = 3.8\,\mu$m and $\lambda = 12.5\,\mu$m, T_c, is given in column 10. In column 11, $W_{9.7}$ is a measure of the relative depth (emission for WX Ser and RS Vir!) of the silicate feature. It is defined as

$$W_{9.7} \equiv \Delta(f_\lambda \Delta\lambda)/S_{\mathrm{IR}}(\mathrm{obs}) \tag{1}$$

expressed in arbitrary units. Here S_{IR}(obs) is the total flux received at the earth, corrected for the missing part at $\lambda > 20\,\mu$m. $\Delta(f_\lambda \Delta\lambda)$ is the total flux absorbed in the 9.7 μm feature. At the same time as the UKIRT observations, OH fluxes were determined with the Dwingeloo Radio Telescope. The absolute integrated flux density at $\lambda = 18$ cm can be found in Column 12.

We were unable to detect four sources at any infrared wavelength, although we had good positions for all of them. OH 0.3–0.2 was detected at $\lambda > 20\,\mu$m only. The same quantities as in Table 2 (as far as applicable) are listed for these undetected stars in Table 3.

It is remarkable that three of the undetected sources appear not to be variable at radio wavelengths (their radio amplitude $\Delta m_r < 3\sigma$, see below; Herman and Habing, 1984a, Table 3), and that the other two have very small amplitude variations. Note that two similar objects in Table 2, OH 31.0–0.2 (non-variable), and OH 17.7–2.0 (slightly variable), both have very steep spectra shortward of the silicate feature. At 3.8 μm and at 4.8 μm they are very weak. Preliminary IRAS survey results of OH 25.1–0.3 indicate also a very red spectrum (Olnon et al., 1984). This suggests that OH/IR stars with small- or zero-amplitude variations are even redder than those with large amplitude variations. Olnon et al. (1984) indeed confirm this effect.

4. Mean luminosities

a) Influence of variability

Besides our radio monitoring program of OH/IR stars one comparable IR program exists. Engels et al. (1983) determined the

Table 2.

Name		P_r (days)	ϕ	D (kpc)	ΔD (kpc)		L_{IR} ($10^4 L_\odot$)	ΔL	T_c (K)	$W_{9.7}$	L_{int} (OH) ($10^{-22} Wm^{-2} kpc^2$)	Remarks
(1)	(2)	(3)	(4)	(5)	(6)	(7)	(8)	(9)	(10)	(11)	(12)	(13)
WX Ser	(a)	443	0.85	1.20	0.55	(1)	0.49	0.32	620	−7.6	7.45	Emission
RS Vir	(a)	364	0.16	0.66	0.05	(1)	0.19	0.02	900	−1.2	3.29	at 9.7 μm
OH 12.8−1.9	(g)	812	0.29	1.69	0.5	(3)	0.59	0.18	580	4.8	86.4	
OH 17.7−2.0	(d)	890:	0.06:	3.17		(4)	0.26		280	3.0	2700	Slightly variable
OH 20.2−0.1	(e)	857	0.96	2.68		(4)	0.78		510	6.5	114	
OH 20.7+0.1	(b)	1130	0.10	8.31	0.82	(2)	0.55	0.08	380	10.8	2240	
OH 21.5+0.5	(b)	1975	0.61	11.63	0.65	(2)	3.42	0.27	360	13.8	4670	
OH 26.2−0.6	(e)	1181	0.50	1.48		(4)	0.088		470	12.5	36.1	
OH 26.4−1.9	(e)	652	0.75	1.54		(4)	0.23		540	6.3	48.6	
OH 28.5−0.0	(b)	559	0.32	2.45		(4)	0.033		420	>15.7	159	
OH 28.7−0.6	(e)	627	0.60	2.40		(4)	0.31		550	5.4	82.7	
OH 30.1−0.7	(b)	2060	0.91	1.77	0.31	(2)	0.39	0.10	410	17.7	551	
OH 30.1−0.2	(f)	853	0.78	1.40	0.4	(3)	0.12	0.05	510	6.6	53.9	
OH 30.7+0.4	(e)	1039	0.15	6.31		(4)	3.16		500	12.3	679	
OH 31.0−0.2	(b)			6.50		(4)	0.76		360	20.6	932	Non variable
OH 32.0−0.5	(b)	1540	0.08	9.30	2.0	(2)	3.68	1.12	450	14.6	4080	
OH 32.8−0.3	(b)	1536	0.39	8.05	0.24	(2)	3.54	0.15	440	>17.0	5690	
OH 39.7+1.5	(d)	1424	0.20	0.57	0.21	(2)	0.25	0.13	520	10.3	61.5	
OH 39.9−0.0	(c)	823	0.98	3.07	0.8	(3)	0.49	0.20	500	9.9	226	
OH 42.3−0.1	(e)	1945	0.03	3.47		(4)	0.35		390	17.4	710	

Positions.

(a) Kukarkin *et al.*, 1969.
(b) VLA position. Herman *et al.*, table 2.
(c) VLA position. B. Baud, private communication.
(d) VLA position. Bowers *et al.*, 1981.
(e) IR position. Jones *et al.*, 1982.
(f) IR position. Engels *et al.*, 1982.
(g) Westerbork position. F. Willems, T. de Jong, private communication.

Distances.

(1) Combination of Robertson and Feast, 1981, Rieu *et al.*, 1979 and K_{abs} (2.2 μm) = $2^m.1$ (at 1 kpc).
(2) Geometric. Herman *et al.*, table 3.
(3) L_{OH}-R_o relation. Herman and Habing, 1984b.
(4) Combination of the near kinematic distance and L_{OH}-R_o relation.

Table 3.

Name		P_r (days)	ϕ	D (kpc)		L_{int} (OH) ($10^{-22} Wm^{-2} kpc^2$)	Remarks
(1)	(2)	(3)	(4)	(5)	(7)	(12)	
OH 0.3−0.2	(c)			9.2	(GC)	1470	Non variable. [20 μm] = $2^m.98$
OH 1.5−0.0	(c)			9.2	(GC)	761	Non variable. Confusion by 'blue' object.
OH 15.7+0.8	(d)			0.3	(4)	6.0	Non variable. Undetected at [3.8], [8.7], and [12.5] within 60" around VLA position.
OH 18.5+1.4	(b)	1125:	0.02:	4.5	(4)	470	Slightly variable ($\Delta m_r \lesssim 0^m.19$). Undetected at [8.7]
OH 25.1−0.3	(b)	226:	0.31:	4.7	(4)	123	Slightly variable ($\Delta m_r \lesssim 0^m.21$). Undetected at [8.7]

OH/IR stars in common with our program. In addition, we combine our luminosities with those of Evans and Beckwidth (1977), and with those of Werner et al. (1980), using the periods and phases as found in the Dwingeloo monitor program (see Fig. 11). We find good agreement between all measurements for OH 21.5+0.5, OH 26.5+0.6, OH 32.8–0.3, and OH 45.5+0.1. The time of maximum for OH 30.1−0.7 is good, but our radio period seems to be somewhat long; probably because we had incomplete coverage of the light curve in the Dwingeloo program (missing the maximum), and the light curve is asymmetric. The luminosities for OH 30.1−0.2 show somewhat larger scatter (±50%). This source, however, is apparently weak, and the three observers covered only the minimum, $\phi = 0.2-0.8$.

We define the amplitude, A, of the variation as $A \equiv L_{max}/L_{min}$; A_L is the ratio for the total luminosity, and A_R that for the radio luminosity in the 18 cm line (1612 MHz). In Table 4 the quantity Δm_r, defined as $\Delta m_r \equiv 2.5 \log A_R$ is listed. For the ratio A_L/A_R the following values are found: 2.05 for OH 21.5+0.5, 2.07 for OH 26.5+0.6, ~1.46 for OH 30.1−0.7, ~1.27 for OH 30.1−0.2, 1.92 for OH 32.8−0.3, and 1.97 for OH 45.5+0.1. So quite speculatively, we derive

$$A_L \simeq 2.0 \; 10^{0.4 \Delta m_r} \tag{2}$$

In other words, the radio amplitude (reflecting the amplitude at 35 μm, see Sect. 7) is only half the amplitude of the bolometric magnitude. We will assume that Eq. (2) holds for all OH/IR stars.

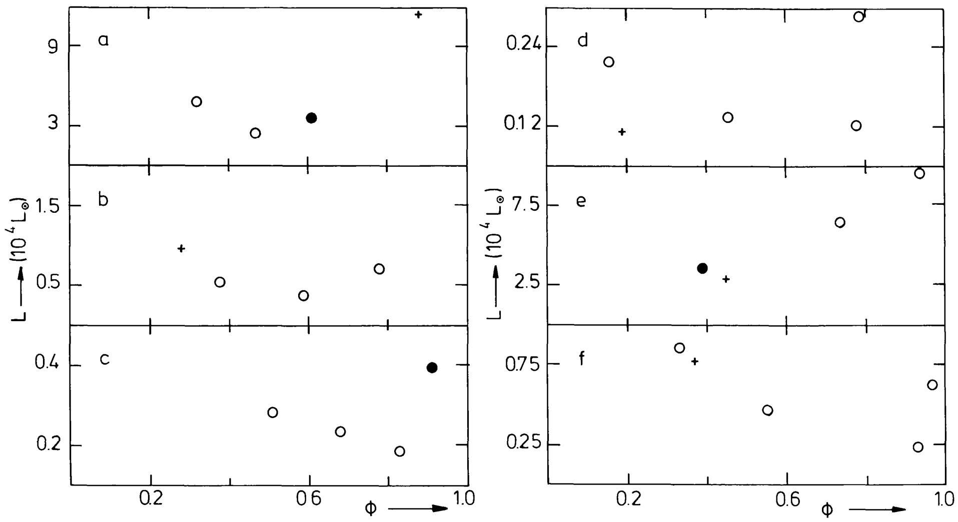

Fig. 11a–f. Variation of the luminosity. Open circles are observations of Evans and Beckwith (1977), crosses those of Werner et al. (1980). Dots are our own observations. **a** OH 21.5+0.1, **b** OH 26.5+0.6, **c** OH 30.1−0.7, **d** OH 30.1−0.2, **e** OH 32.8−0.3, and **f** OH 45.5+0.1

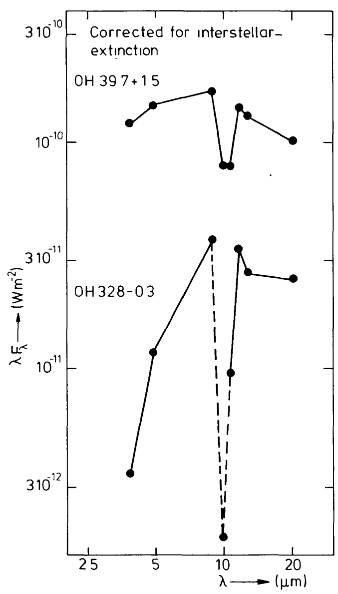

Fig. 12. Example of two spectra corrected for interstellar extinction (cf. Fig. 9). OH 32.8−0.3 is far away ($D = 8$ kpc), OH 39.7+1.5 nearby ($D = 0.57$ kpc)

Furthermore, we assume that the luminosity varies sinusoidally. Although we know that, in general, the light curves are asymmetric (Herman and Habing, 1984a), this assumption will hardly affect our results. We may then write for the mean luminosity

$$L_M = D^2 S_{\mathrm{IR}}(\mathrm{obs})\,\{1 + \cos(2\pi\phi_{\mathrm{obs}})\,[A_L - 1]\,[A_L + 1]^{-1}\}^{-1} \tag{3}$$

where $D^2 S_{\mathrm{IR}}(\mathrm{obs}) = L_{\mathrm{IR}}$, the values listed in Table 2.

b) Influence of interstellar extinction

Although the interstellar extinction at infrared wavelengths is mostly regarded as *quantité négligeable*, we will nevertheless correct for it, because the OH/IR stars are at low galactic latitudes and at large distances from the Sun. Adopting the model advocated by de Jong (1983) we write for the extinction coefficient

$$\begin{aligned} \kappa(R,z) &= \kappa_0 \left(\frac{R_0}{R}\right)^2 \exp\left(-\frac{z}{z_g}\right) \quad \text{for} \quad R \geqq R_m \\ &= 1.5\kappa_0 \exp\left(-\frac{z}{z_g}\right) \quad \text{for} \quad R < R_m\,, \end{aligned} \tag{4}$$

where $\kappa_0 = 1.6\,\mathrm{mag\,kpc^{-1}}$ is the local extinction coefficient (Greenberg, 1968), R is the galacto-centric distance, $R_\odot = 9.2$ kpc, and $z_g = 60$ pc is the scale height of the molecular gas in the galaxy (Solomon et al., 1979). $R_m = 3.7$ kpc is the inner radius of the molecular gas ring (Gordon and Burton, 1976). Integration along the line of sight to an object yields the visual extinction, A_v. Then, using the wavelength dependence of the interstellar extinction in the infrared (Beckling et al., 1978), we can calculate the corrected infrared fluxes (see for an example Fig. 12; cf. Fig. 9) and the corrected mean luminosities, L_M^c. The results can be found in Table 4, where in Column 2 the mean luminosities [from Eq. (3)] are listed. Column 3 gives the visual extinctions, A_v, and column 4 the resulting corrected mean luminosities, L_M^c. The mean of the integrated OH flux density is listed in Column 5; the radio amplitudes (Δm_r) and the expansion velocities of the OH shell (v_e), all from Herman and Habing (1984a), are tabulated in Columns 6 and 7.

Note that there are only six stars in Table 4 with mean luminosities larger than $10^4\,L_\odot$. The others lie in the luminosity range of the normal Mira variables (cf. Eggen, 1975). This is in good agreement with the statistical results of Jones et al. (1982). We also find that the sources with large expansion velocities ($v_e > 15\,\mathrm{km\,s^{-1}}$), that are thought to be the younger and more massive stars (see Baud et al., 1981), are more luminous, $\langle L_M^c \rangle = 2.82\,10^4\,L_\odot$, than the OH/IR stars with small expansion velocities, $\langle L_M^c \rangle = 0.53\;10^4\,L_\odot$, as suggested by Fig. 13. Two objects, OH 21.5+0.5 and OH 32.8−0.3, have luminosities in excess of the asymptotic giant branch limit ($\sim 5\;10^4\,L_\odot$; see Iben, 1981), even without correction for the interstellar extinction. Their geometrically determined distances are quite accurate. Therefore, they should be identified with supergiants. Notice, however, their large radio amplitudes, quite contrary to the small amplitudes of the optically identified supergiants (Herman and Habing, 1984a, Table 2).

Table 4.

Name (1)	L_M (10^4 $L_\odot$) (2)	A_V (mag) (3)	L_M^c (10^4 $L_\odot$) (4)	$\bar{L}_{int}$ (10^{-22}Wm^{-2}kpc^2) (5)	Δm_r (mag) (6)	v_e (km s^{-1}) (7)	Remarks (8)
WX Ser	0.37	0.02	0.37	6.69	0.58	7.59	
RS Vir	0.15	0.02	0.15	3.14	0.48	4.29	
OH 12.8-1.9	0.69	2.02	0.73	124	0.56	22.61	
OH 17.7-2.0	0.19	2.87	0.21	2460	0.16	12.89	Slightly variable.
OH 20.2-0.1	0.50	5.54	0.59	117	0.67	16.45	
OH 20.7+0.1	0.36	29.47	0.92	1680	0.99	18.21	
OH 21.5+0.5	7.32	20.66	14.05	7670	1.09	18.76	L_M based also on observations of EB and W.
OH 26.2-0.6	0.27	2.35	0.29	89.2	1.05	22.11	
OH 26.4-1.9	0.23	1.79	0.25	55.6	0.44	12.09	
OH 26.5+0.6	0.94	1.53	1.00	615	1.13	14.07	L_M based on EB and W. P = 1560^d; D = 0.98 kpc
OH 28.5-0.0	0.044	5.01	0.049	158	0.77	13.12	
OH 28.7-0.6	0.63	3.10	0.69	129	0.83	17.38	
OH 30.1-0.7	0.32	2.74	0.35	621	0.40	20.51	L_M based also on EB and W.
OH 30.1-0.2	0.19	2.44	0.20	75.0	0.81	17.60	L_M based also on EB and W.
OH 30.7+0.4	1.20	13.31	1.82	459	0.57	17.24	
OH 31.0-0.2	0.76	17.30	1.31	946	<0.13	14.26	Non variable.
OH 32.0-0.5	2.36	18.47	4.22	2820	0.88	20.58	
OH 32.8-0.3	7.34	20.46	14.02	6590	1.24	16.38	
OH 39.7+1.5	0.21	0.80	0.22	54.4	0.82	16.58	
OH 39.9-0.0	0.30	6.47	0.37	183	0.80	14.71	
OH 42.3-0.1	0.24	7.03	0.30	597	0.36	16.37	
OH 45.5+0.1	0.85	7.34	1.08	191	0.92	17.13	L_M based on EB and W. P = 761^d; D = 3.65 kpc.

EB: Evans and Beckwith, 1977.
W: Werner *et al.*, 1980.

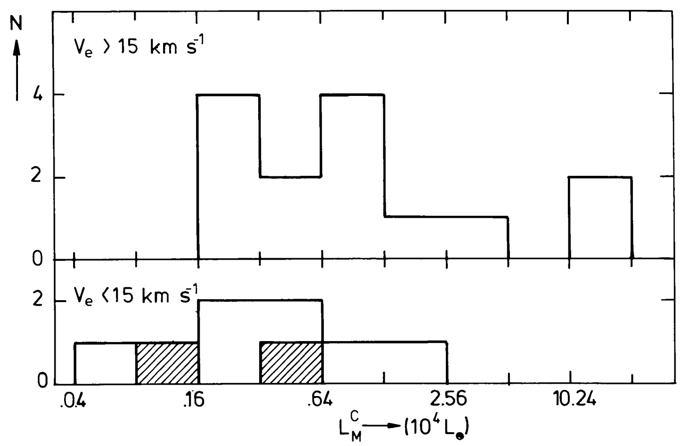

Fig. 13. Distribution of the mean corrected luminosities for our heterogeneous sample, divided into objects with small ($v_e < 15\,\mathrm{km\,s^{-1}}$) and large $v_e > 15\,\mathrm{km\,s^{-1}}$) expansion velocities of the circumstellar envelope. The two Mira variables are shaded

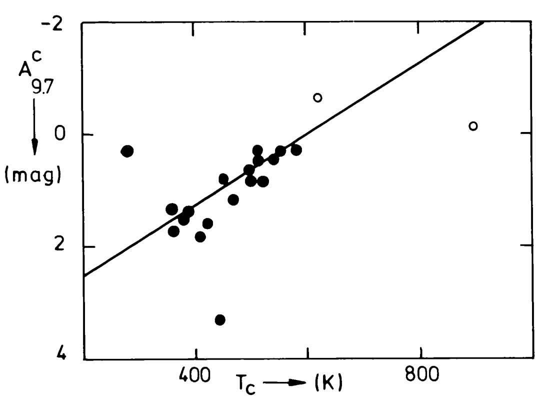

Fig. 14. Depth of the silicate feature, $A^c_{9.7}$ (corrected for interstellar extinction), as function of the colour temperature, T_c. The drawn line is the expected slope from $\tau_{sil} \sim T_c^{-1}$ (Kwan and Scoville, 1976)

5. The 9.7 μm feature

The absorption or emission feature at 9.7 μm seen in oxygen-rich stars is normally attributed to stretching and bending vibrations in silicate materials (see Merrill, 1977). A considerable fraction of this feature is formed in the circumstellar dust shell, and it is certainly not dominated by intervening material somewhere else along the line of sight. Evans and Beckwith (1977) give a number of arguments for this proposition, the strongest being the total lack of correlation between the distance and the depth of the absorption feature (cf. also Table 2), and the positive correlation found (for six stars only) between the colour temperature, T_c, and the relative depth of the absorption feature, $A^c_{9.7}$ (see also Fig. 14), where

$$A^c_{9.7} \equiv -2.5 \log (I^c_{cont}/I^c_{9.7}) \quad (5)$$

is corrected for interstellar extinction. Our slope is in agreement with the suggested correlation between $\tau_{sil}(\sim A_{9.7})$ and T_c^{-1} (Kwan and Scoville, 1976), based on a simple model of radiative transport (Table 5).

Note that the two Mira variables, where the silicate feature is seen in emission, have the highest colour temperatures. Only two OH/IR stars deviate substantially from the mean relation; the extremely cool shell of OH 17.7−2.0 hardly shows absorption at 9.7 μm, suggesting that the temperature gradient is small in this presumably very thick envelope, and OH 32.8−0.3 has a very deep absorption feature (see also Table 5). As this star is far away (its geometric distance is 8.05 kpc), large deviations from the simple, uniform extinction model may account for this discrepancy. Also, it has been found (Forrest et al., 1978) that in OH 26.5+0.6 the silicate absorption feature is deeper when the star is fainter, and we observed OH 32.8−0.3 near minimum light ($\phi = 0.39$).

It is clear from Fig. 15 that the depth of the silicate feature, which is primarily a measure of the amount of cold material in the envelope, is correlated with the fraction of the total luminosity that is converted, via the far infrared pump cycle, into OH luminosity at 18 cm. As $A_{9.7}$ increases (i.e. the colour temperature decreases) more pump photons are produced, and the relative OH strength increases. This confirms that the OH masers are pumped by far

Table 5.

Name	$A_{9.7}$ (mag)	$A^c_{9.7}$ (mag)	Name	$A_{9.7}$ (mag)	$A^c_{9.7}$ (mag)
(1)	(2)	(3)	(1)	(2)	(3)
WX Ser	-0.65	-0.65	OH 28.7-0.6	0.44	0.30
RS Vir	-0.10	-0.10	OH 30.1-0.7	2.02	1.81
OH 12.8-1.9	0.35	0.32	OH 30.1-0.2	0.57	0.44
OH 17.7-2.0	0.35	0.30	OH 30.7+0.4	1.54	0.81
OH 20.2-0.1	0.68	0.30	OH 31.0-0.2	2.38	1.33
OH 20.7+0.1	5.65	1.51	OH 32.0-0.5	2.01	0.82
OH 21.5+0.5	3.15	1.75	OH 32.8-0.3	>4.62	>3.31
OH 26.2-0.6	1.30	1.17	OH 39.7+1.5	0.94	0.88
OH 26.4-1.9	0.47	0.44	OH 39.9-0.0	0.96	0.63
OH 28.5-0.0	>1.90	>1.59	OH 42.3-0.1	1.81	1.37

ad. (2), (3): positive values indicate absorption at 9.7 µm.
ad. (3): corrected for interstellar extinction.

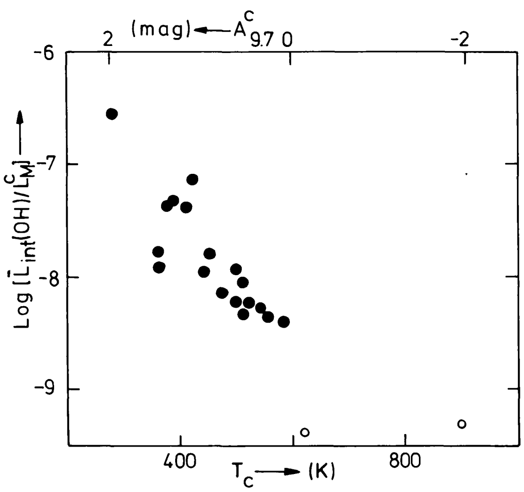

Fig. 15. Fraction of the total luminosity that is converted into OH luminosity at 1612 MHz as function of colour temperature, or depth of the silicate feature

infrared photons (Elitzur et al., 1976; see also Sect. 7). Furthermore, because the OH luminosity also depends on the velocity field and on the fraction of H_2O molecules that are photodissociated into OH (see Herman and Habing, 1984a), the relatively small scatter in Fig. 15 indicates that for this sample (a selection of only *strong* OH emitters, apart from the two Mira variables) these quantities are roughly the same.

6. The colour temperatures

It was shown in the previous section that the colour temperature, T_c, is inversely proportional to the depth in the silicate feature (Fig. 14), in agreement with theoretical predictions by Kwan and Scoville (1976). These authors also suggest that the colour temperature will change when the luminosity varies: $T_c \sim L^x$, where $x = 0.25 - 0.20$ for an emissivity dependence of the dust $\sim \lambda^0$ and $\sim \lambda^{-1}$, respectively. The combination of our observations with those of Evans and Beckwith (1977), and with those of Werner et al. (1980) provides a sufficiently long time scale for these slowly varying stars to permit an analysis of the changes in T_c (see Fig. 16).

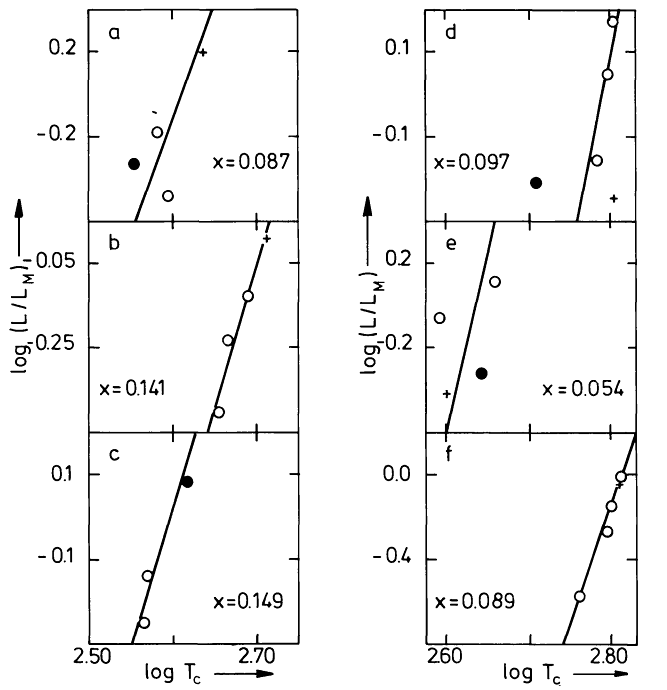

Fig. 16a–f. Variation of the colour temperature, T_c. Open circles are observations of Evans and Beckwith (1977), crosses those of Werner et al. (1980). Dots are our own observations. **a** OH 21.5+0.5, **b** OH 26.5+0.6, **c** OH 30.1−0.7, **d** OH 30.1−0.2, **e** OH 32.8−0.3, and **f** OH 45.5+0.1

We find $\langle x \rangle = 0.103 \pm 0.015$, significantly less than the theoretical prediction. Two remarks should be made: in the first place, the analysis of Kwan and Scoville was for two pre main-sequence objects, where the density distribution of the dust seems to be proportional to r^{-1}, whereas a density fall-off of r^{-2}, or steeper, was found (Herman et al., 1984) for the evolved stars; in the second place, the variation in temperature of the dust, and hence in T_c, may lag behind changes in luminosity. Due to the sparse phase coverage we cannot take such an effect into account. Nevertheless, although the uncertainties are still very large, it seems that the value of x is definitely smaller than the theoretical value of 0.2 (see also Elitzur et al., 1976).

7. Maser pump

OH masers are pumped radiatively by infrared photons (see Harvey et al., 1974). The first pumping scheme proposed involved excitation of the OH molecules to the first vibrational level at 2.8 µm (Litvak, 1969). In view of the very low fluxes of OH/IR stars at $\lambda = 2.8$ µm this scheme might only work for the Mira variables (see Fig. 17 and Evans and Beckwith, 1977). Later, a scheme was developed involving rotational excitation at 35 µm, and to a lesser extent at 53 µm (Elitzur et al., 1976; Bujarrabal et al., 1980), with a predicted efficiency of ~25%. Werner et al. (1980) have shown that the observations of OH/IR stars are in agreement with this prediction. The efficiency, ε, is defined simply as the fraction of 35 µm photons that are converted into OH photons; Evans and Beckwith (1977) have shown that, to first approximation, we may write

$$\varepsilon \equiv \frac{S_\nu(\mathrm{OH})}{S_\nu(35\,\mu\mathrm{m})} = \frac{L(\mathrm{OH})}{L(35\,\mu\mathrm{m})}, \quad (6)$$

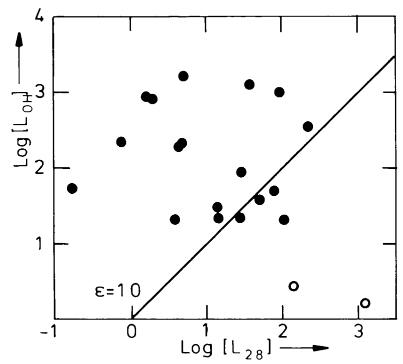

Fig. 17. OH power density (Jy kpc^2) at 1612 MHz as function of the power density (Jy kpc^2) at 2.8 μm (same phase). Open circles represent the Mira variables, filled circles the OH/IR stars. The area to the left on the drawn line is "forbidden" if the 2.8 μm pumping scheme is to work

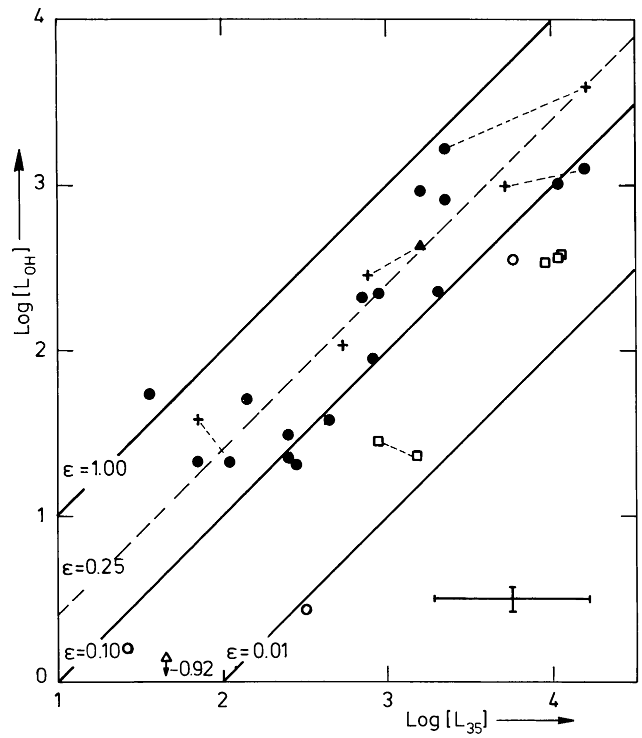

Fig. 18. OH power density (Jy kpc^2) at 1612 MHz as function of the power density (Jy kpc^2) at 35 μm (same phase). Open symbols represent optically identified masers (triangle and squares are IR observations by Forrest et al., 1979), filled symbols the OH/IR stars (crosses: Werner et al., 1980; triangle, Forrest et al., 1979). Measurements of the same object at different epochs are connected by dotted lines. The dashed line is the predicted pump efficiency, $\varepsilon = 0.25$ (Elitzur et al., 1976)

where S_ν(OH) and S(35 μm) are the simultaneously measured flux densities in Jy. We used $L(\mathrm{OH}) = D^2\{S_L \cdot S_H\}^{1/2}$, the harmonic mean of the two strongest (low- and high-velocity) peaks in the OH line profile and determined the flux at 35 μm from an extrapolation of the spectra, corrected for interstellar extinction, between $\lambda = 12.5$ μm and $\lambda = 20$ μm. The latter method is very uncertain and can introduce errors of a factor 3, but we included also the much more accurate measurements of Forrest et al. (1979), and those of Werner et al. (1980), combined with the OH fluxes at the appropriate phase (see Fig. 18). Despite the uncertainties only one object (OH 28.5 − 0.0) falls in the "forbidden" region with $\varepsilon > 1$, and the OH/IR stars lie reasonably close to the predicted value $\varepsilon = 0.25$. Note that the pump efficiency is roughly constant for measurements at different phases, as expected in saturated masers. We find for the OH/IR stars a mean pump efficiency $\langle\varepsilon\rangle = 0.30 \pm 0.06$, so that three to four 35 μm photons are needed to produce one maser photon. The standard deviation is me = 0.31 (factor 2). For the two supergiants we find $\langle\varepsilon\rangle = 0.030 \pm 0.004$, and for the three Mira variables $\langle\varepsilon\rangle = 0.030 \pm 0.004$, an order of magnitude less than for the OH/IR stars. Rieu et al. (1979; see also Bujarrabal et al., 1980) worked out a more detailed model in which they account for velocity gradients in the envelopes and far infrared line overlap. These gradients only marginally affect the OH/IR stars with their very thick dust shells, but for the OH Mira's with thin dust shells an upper limit to the 35 μm pump efficiency of $\varepsilon < 0.1$ is deduced. A low efficiency may also apply to the supergiants, as these have rather thin envelopes. It is interesting that VLBI measurements of some supergiants (Benson and Mutel, 1979) were not compatible with the simple geometry of an expanding shell, suggesting that in these objects larger velocity gradients might be present.

8. Conclusions

New infrared photometric measurements have provided good absolute luminosities for a large sample of OH/IR stars. A reasonable estimate of the mean luminosities of these objects has also been derived. A third of our objects has large luminosities, in excess of $10^4\,L_\odot$; most of the other luminosities are comparable to, though slightly larger than, the classical Mira variables. But remember that the sources in our sample have been selected because they are "radio bright", and therefore had accurately known radio positions. The near infrared colour temperatures, the depth of the silicate feature, and the fraction of luminosity converted into OH luminosity, are correlated. Lower T_c implies thicker dust shells, deeper silicate absorption features, and stronger maser emission. Detailed confirmation of the far infrared pumping scheme for 1612 MHz OH masers awaits direct measurements of the 35 μm flux.

We were unable to detect some OH sources at near infrared wavelengths in spite of the very good radio positions. Together with two stars that were only marginally detectable at the shorter infrared wavelengths, these objects seem to be of a different mold than the other OH/IR stars; either they do not vary at all, or if they do, they have very small amplitudes. Interestingly, these stars also appear to have small angular sizes; they were unresolved with the VLA (Herman et al., 1984). Hence they are either very far away, $D \gtrsim 8$ kpc, or rather close, $D \lesssim 2$ kpc, and consequently low mass stars with extraordinary large mass loss rates (Herman and Habing, 1984b). IRAS observations indicate that OH/IR stars with small variations are indeed significantly redder than those with large radio amplitudes (Olnon et al., 1984), confirming the latter possibility.

Acknowledgements. We wish to thank Dr. I. Gatley for his valuable assistance with the observations. The UKIRT facility is run on behalf of the United Kingdom Science Research Council from the Royal Observatory, Edinburgh. J. Herman was supported by a grant from ASTRON, the Netherlands Foundation for Radio Astronomy. ASTRON receives its funds from Z.W.O., the Netherlands Organization for the Advancement of Pure Research.

Table A1

Name \ Band λ(μm)	L' 3.8	M 4.8	N_1 8.7	N_2 9.7	N_3 10.5	N_4 11.5	N_5 12.5	Q 20	Largest error	Band
WX Ser	0.88	0.40	-1.40	-1.90	-1.98	-2.06	-1.94	-3.15	0.05	N_1
RS Vir	0.03	-0.21	-1.18	-1.45	-1.55	-1.64	-1.65	-2.28	0.07	N_1
OH 12.8-1.9	1.73	0.99	-0.85	-0.80	-1.14	-1.67	-1.72	-2.67	0.07	N_5
OH 17.7-2.0	7.06	5.90	2.17	1.85	1.30	0.32	-0.14	-2.58	0.08	M
OH 20.2-0.1	3.00	2.24	-0.08	0.31	0.17	-0.49	-0.77	-1.28	0.06	N_3
OH 20.7+0.1	8.12	5.13	3.24	3.97	4.70	2.06	1.07	-0.36	0.15	N_3
OH 21.5+0.5	7.48	4.69	2.11	4.50	4.40	1.34	0.10	-0.61	0.14	N_2
OH 26.2-0.6	4.30	2.99	0.85	1.80	1.55	0.06	-0.22	-1.25	0.08	Q
OH 26.4-1.9	3.09	1.90	-0.08	0.11	0.07	-0.74	-0.94	-2.23	0.04	N_5
OH 28.5-0.0	7.64	5.41	3.09	>4.5	>4.5	2.53	1.56	0.56	0.11	Q
OH 28.7-0.6	3.30	2.50	0.62	0.73	0.45	-0.14	-0.29	-1.78	0.06	N_3
OH 30.1-0.7	4.03	8.33	-0.50	1.09	0.66	-1.11	-1.65	-3.17	0.12	N_2
OH 30.1-0.2	3.34	2.42	0.54	0.72	0.49	-0.30	-0.58	-1.74	0.03	N_4
OH 30.7+0.4	3.73	2.06	0.34	1.46	1.21	-0.41	-0.96	-2.31	0.06	N_2
OH 31.0-0.2	7.77	4.86	1.56	3.53	3.29	1.17	0.30	-1.06	0.09	N_3
OH 32.0-0.5	4.96	3.01	1.01	2.40	1.95	0.16	-0.49	-1.95	0.06	N_2
OH 32.8-0.3	5.14	2.82	0.77	>4.8	2.37	0.08	-0.81	-2.45	0.07	N_3
OH 39.7+1.5	0.52	-0.42	-2.42	-1.89	-2.16	-3.15	-3.36	-4.56	0.05	N_2
OH 39.9-0.0	3.90	2.60	0.62	1.23	1.11	-0.12	-0.37	-1.79	0.05	N_2
OH 42.3-0.1	5.87	3.97	1.08	2.47	2.33	0.35	-0.16	-1.47	0.11	N_2

Table A2

Standard \ Band λ(μm)	L' 3.8	M 4.8	N_1 8.7	N_2 9.7	N_3 10.5	N_4 11.5	N_5 12.5	Q 20	
α Sco		-3.84	-4.55	-4.60	-4.64	-4.77	-4.76	-4.70	BS 6134
α Boo		-2.95	-3.17	-3.22	-3.15	-3.23	-3.33	-3.30	
β Peg	-2.34	-2.21	-2.45	-2.56	-2.55	-2.59	-2.70	-2.90	BS 8775
BS 6406		-3.44	-3.84	-3.89	-3.87	-4.05	-4.16	-4.30	

Appendix A. Results of the infrared observations at UKIRT

Table A1 gives the magnitudes in each band for all stars in our program that were detected. The precise wavelengths and widths of the bands, and the conversion factors of magnitudes to Jansky's can be found in the text (Sect. 2, Table 1). The uncertainties in the tabulated magnitudes are typically $0^{\rm m}05$. For each source the largest error, and the band in which that occurs, is listed. Before and after an observation of a program star, standard stars were observed, allowing a good air mass correction and flux calibration. In Table A2 these standards are listed with the magnitudes adopted for each band.

Some other bright stars (BS, or HR catalogue) were used for the *L*'band. They were (with their magnitude at $L' = 3.8$ μm between brackets): BS 4689 ($3^{\rm m}76$), BS 5200 ($0^{\rm m}20$), BS 5447 ($3^{\rm m}44$), BS 6746 ($0^{\rm m}65$), BS 7120 ($1^{\rm m}90$), and BS 8167 ($2^{\rm m}13$).

References

Baud, B., Habing, H.J., Winnberg, A., Matthews, H.E.: 1981, *Astron. Astrophys.* **95,** 156

Becklin, E.E., Matthews, K., Neugebauer, G., Willner, S.P.: 1978, *Astrophys. J.* **220,** 831

Beckwith, S., Evans II, N.J., Becklin, E.E., Neugebauer, G.: 1976, *Astrophys. J.* **208,** 390

Benson, J.M., Mutel, R.L.: 1979, *Astrophys. J.* **233,** 119

Bowers, P.F., Johnston, K.J., Spencer, J.H.: 1981, *Nature* **291,** 382

Bujarrabal, V., Quibert, J., Rieu, Nguyen-Q., Omont, A.: 1980, *Astron. Astrophys.* **84,** 311

Eggen, O.J.: 1975, *Astrophys. J.* **195,** 661

Engels, D.: 1982, Zur Natur von OH/IR-Objekten, Ph. D. Thesis, Veröff. Astron. Inst. Bonn **95**

Engels, D., Kreysa, E., Schultz, G.V., Sherwood, W.A.: 1983, *Astron. Astrophys.* **124,** 123

Elitzur, M.: 1981, in *Physical Processes in Red Giants*, eds. I. Iben, A. Renzini, Reidel, Dordrecht, pp. 363–382

Elitzur, M., Goldreich, P., Scoville, N.: 1976, *Astrophys. J.* **205,** 384

Evans, N.J., Beckwith, S.: 1977, *Astrophys. J.* **217,** 729

Forrest, W.J., Gillett, F.C., Houck, J.R., McCarthy, J.F., Merrill, K.M., Pipher, J.L., Puetter, R.C., Russell, R.W., Soifer, B.T., Willner, S.P.: 1978, *Astrophys. J.* **219,** 114

Forrest, W.J., McCarthy, J.F., Houck, J.R.: 1979, *Astrophys. J.* **233,** 611

Gordon, M.A., Burton, W.B.: 1976, *Astrophys. J.* **208,** 346

Greenberg, J.M.: 1968, in *Stars and Stellar Systems*, eds. B.M. Middlehurst and L.H. Aller, Vol. **VII,** p. 221

Harvey, P.M., Bechis, K.B., Wilson, W.J., Ball, J.A.: 1974, *Astrophys. J. Suppl.* **27,** 331

Herman, J., Habing, H.J.: 1984a, *Astron. Astrophys.*, submitted see Herman, J., Ph. D. Thesis, RUL, 1983, Chap. II

Herman, J., Habing, H.J.: 1984b, see Herman, J., Ph. D. Thesis, RUL, 1983, Chap. V (in preparation)

Herman, J., Baud, B., Habing, H.J., Winnberg, A.: 1984, *Astron. Astrophys.*, submitted see Herman, J., Ph. D. Thesis, RUL, 1983, Chap. III

Hyland, A.R., Becklin, E.E., Frogel, J.A., Neugebauer, G.: 1972, *Astron. Astrophys.* **16,** 204

Iben, I.: 1981, in *Physical Processes in Red Giants*, eds. I. Iben, A. Renzini, Reidel, Dordrecht, pp. 3–24

Johnson, H.L.: 1966, in *Ann. Rev. Astron. Astrophys.* **4,** 193

Jong, T. de: 1983, *Astrophys. J.* **274,** 252

Jones, T.J., Ashley, M., Hyland, A.R., Ruelas-Mayorga, A.: 1981, *Monthly Notices Roy. Astron. Soc.* **197,** 413

Jones, T.J., Hyland, A.R., Caswell, J.L., Gatley, I.: 1982, *Astrophys. J.* **253,** 208

Jones, T.J., Hyland, A.R., Wood, P.R., Gatley, I.: 1983, *Astrophys. J.* **273,** 669

Kukarkin, B.V., Kholopov, P.N., Efremov, Yu.N., Kukarkina, N.P., Kurochkin, N.E., Medvedeva, G.I., Perova, N.B., Fedorovich, V.P., Frolov, M.S.: 1969, General Catalogue of Variable Stars, Moscow (+ Supplements)

Litvak, M.M.: 1969, *Astrophys. J.* **156,** 471

Kwan, J., Scoville, N.: 1976, *Astrophys. J.* **209,** 102

Merrill, K.M.: 1977, in The Interaction of Variable Stars with their Environment, eds. R. Kippenhahn, J. Rahe, W. Strohmeier, Veröff. Remeis Sternwarte, Bamberg, Bd. XI, Nr. 121, p. 446

Olnon, F.M., Baud, B., Habing, H.J., de Jong, T., Harris, S., Pottasch, S.R.: 1984, *Astrophys. J. Letters* **278,** L41

Rieu, Nguyen-Q., Laury-Micolaut, C., Winnberg, A., Schultz, G.K.: 1979, *Astron. Astrophys.* **75,** 351

Robertson, B.S.C., Feast, M.W.: 1981, *Monthly Notices Roy. Astron. Soc.* **196,** 111

Solomon, P.M., Sanders, D.B., Scoville, N.Z.: 1979 *IAU Symp.* **84,** ed. W.B. Burton, p. 35

Wamsteker, W.: 1981, *Astron. Astrophys.* **97,** 329

Werner, M.W., Beckwith, S., Gatley, I., Sellgren, K., Berriman, G., Whiting, D.L.: 1980, *Astrophys. J.* **239,** 540